Inelastic cross sections, overlap functions and C_q moments from ISR to LHC energies in proton interactions

P.C. Beggio

Laboratório de Ciências Matemáticas - LCMAT,

Universidade Estadual do Norte Fluminense Darcy Ribeiro - UENF,

28013-602, Campos dos Goytacazes, RJ, Brazil

arXiv:1701.08574v1 [hep-ph] 30 Jan 2017

Abstract

We investigated the energy dependence of the parton-parton inelastic cross sections, parton-parton inelastic overlap functions and the C_q moments in proton interactions from $\sqrt{s}$= 10 to 14000 GeV. The used approach is based on a phenomenological procedure where elastic and inelastic proton observables are described in a connected way by exploring the unitarity of S-Matrix. Applying a Quantum Chromodynamics inspired eikonal model, that contains contributions of the quark-quark, quark-gluon and gluon-gluon interactions, theoretical predictions on inelastic cross sections and C_q moments are compared with measurements showing successfully description of the experimental data. The KNO hypothesis violation is discussed as a consequence of the semihard contribution to the multiparticle production in the interactions, in accordance to several experimental and theoretical previous results. Prediction to the ratio σ_{el}/σ_{tot} as a function of the collision energy is presented and also compared with the experimental information.

I. INTRODUCTION

In the nonperturbative sector of Quantum Chromodynamics - QCD - one of the problems is the hadronization mechanism and the probability for producing the number n of charged hadrons in the final state of proton collisions, P_n, is a very important physical observable to investigate the multiparticle production dynamics sector, providing important insigths on the particle production mechanisms. The multiplicity distribution is defined as $P_n = \sigma_n/\sigma_{in}$, where σ_n and σ_{in} are the topological and inelastic cross sections, respectively. The cross sections, and hence P_n, cannot yet be calculated from QCD. Thus, our knowledge on multiparticle production dynamics is still phenomenological and based on a wide class of models [1] and some theoretical principles. In particular the unitarity principle is very important in the nonperturbative sector, which regulates the relative strength of elastic and inelastic processes [2]. We note that the Froissart-Martin bound on the high energy behavior of total cross section, σ_{tot}, first derived by Froissart from the Mandelstam representation [3] and then proved directly by Martin using unitarity and analycity [4], has been extended to the σ_{in}, also implying that the σ_{in} cannot rise faster than $ln^2(s)$ [5].

From experimental side, LHC data on both σ_{in} and charged particle multiplicity moments, in restrict pseudorapidity intervals, are available by CMS, ATLAS, ALICE, TOTEM and LHCb experiments [6] [7] [8] [9] [10] [11] [12] [13]. In addition, there are experimental results on these quantities at lower center-of-mass energy, $\sqrt{s}$, in both restrict and full phase space pseudorapidity intervals obtained by ABCDWH, UA5 and E735 Collaborations [14] [15] [16] [17] [18] [19] [20]. Nowdays, the understanding of the rise of σ_{in} with $\sqrt{s}$, as well as P_n, are of fundamental importance for hadron collider physics, particle astrophysics [7] and also for multiparticle production dynamics sector of QCD [21] [22]. For these reasons, it is important to look for approaches and to test calculation schemes able to describe, in an unified way, elastic and inelastic physical observables in the wide interval of $\sqrt{s}$ covered by experiments. It can give us the chance to quantify the most important trends of the experimental points, as well as indicating for new possible theoretical developments.

In the present work we applied a phenomenological procedure where the connection between elastic and inelastic channels is established through the unitarity condition using the eikonal approximation [23] [24]. We have adopted a QCD-inspired eikonal function [25] in order to investigate the approximate collision energy dependence of the quark-quark, quark-

gluon and gluon-gluon of both, inelastic overlap functions and inelastic cross sections. In the present analysis all parameters of the eikonal has been determined carrying out a global fit to all high energy forward pp and $p\overline{p}$ scattering data above $\sqrt{s}$=10 GeV [25]. We give also quantitative results on the $\sqrt{s}$ dependence of the C_q moments of P_n. The mentioned phenomenological procedure is here referred to as Geometrical Approach and it has permitted some previous studies involving the hadronic physics [24] [26] [27] [28] [29].

The paper is organized as follows: in the next section we present the main equations of the Geometrical Approach, which is composed by the two models, the QCD motivated eikonal dynamical gluon mass model (elastic channel) and the string model (inelastic channel). Motivated by the previous good results obtained by using the approach [25], in Section III we present the strategy used to calculate the partonic and total inelastic overlap function as well as the partonic and total inelastic cross sections. In the sequence we calculate the Cq moments of the multiplicity distributions discussing our main results. In Section IV we draw our conclusions.

II. GEOMETRICAL APPROACH

The approach treats the protons as composite and extended objects and, hence, the impact parameter b is used as an essential variable in the description of the collisions [24] [26] [27], where the impact parameter denotes the distance between the centers of the colliding composite systems in the plane perpendicular to the beam direction [30]. For the sake of discussions we presented here the main equations of the approach, discussed in details in [25]. The $\chi_I(s,b)$ represents the imaginary eikonal and it has been obtained from a QCD-inspired eikonal model which is completely determined only by elastic fit and incorporates soft and semihard process using a formulating compatible with analyticity and unitarity principles. This eikonal model is referred to as Dynamical Gluon Mass (DGM) model [31] [32] [33] and it has been written in terms of even and odd eikonal parts, connected by crossing symmetry, and this combination reads

$$\chi^{\overline{p}p}_{pp}(s,b) = \chi^{+}(s,b) \pm \chi^{-}(s,b)\,. \tag{1}$$

The odd eikonal is written to account on the difference between pp and $p\overline{p}$ channels at low energies and it is simply

$$\chi^{-}(s,b) = C^{-} \sum \frac{m_g}{\sqrt{s}} e^{i\pi/4} W(b;\mu^{-}). \tag{2}$$

$W(b;\mu_{ij})$ is the overlap density for the partons at impact parameter b, $(i,j = q,g)$ and $m_g = 364\ MeV$ is an infrared gluon scale mass [34]. In Eq. (1) the even eikonal is written as the sum of quark-quark, quark-gluon and gluon-gluon contributions

$$\chi^{+}(s,b) = \chi_{qq}(s,b) + \chi_{qg}(s,b) + \chi_{gg}(s,b)\,. \tag{3}$$

The functions $\chi_{qq}(s,b)$ and $\chi_{qg}(s,b)$ are needed to describe the lower energy experimental points and, based on the Regge phenomenology, it has been parametrized as

$$\chi_{qq}(s,b) = i\Sigma\, A\, \frac{m_g}{\sqrt{s}} W(b;\mu_{qq}), \tag{4}$$

and

$$\chi_{qg}(s,b) = i\Sigma \left[A' + B'\, \ln\left(\frac{s}{m_g^2}\right) \right]\, W(b;\mu_{qg}). \tag{5}$$

The Σ factor is defined as $\Sigma = 9\pi\bar{\alpha}_s^2(0)/m_g^2$, being $\bar{\alpha}_s$ and m_g non-perturbative quantities. At higher energies the perturbative component of the DGM model is dominated by gluons with a very small fractional momentum and it is given by

$$\chi_{gg}(s,b) = \sigma_{gg}(s) W(b;\mu_{gg})\,. \tag{6}$$

From the last equation we can see that the energy dependence of $\chi_{gg}(s,b)$ comes from the gluon-gluon cross section, $\sigma_{gg}(s)$, which gives the main contribution to the asymptotic behavior of parton-parton total cross sections. In DGM model formulation the gluon-gluon cross section has been obtained from QCD parton model perturbative cross section for parton pair colliding, also used in some previous works [35] [36] [37] [38]. Thus, defining the variable $\tau = x_1 x_2 = \hat{s}/s$ we can obtain

$$\sigma_{gg}(s) = \int_0^1 d\tau \left[\int\int g(x_1)\, g(x_2)\, \delta(\tau - x_1 x_2)\, dx_1 dx_2 \right]\, \hat{\sigma}_{gg}(\hat{s})\, \Theta(\hat{s} - m_g^2), \tag{7}$$

where x_i is the fraction of the momentum of the proton carried by gluon i, the factor $\hat{\sigma}_{gg}(\hat{s})$ is the total cross section for the subprocess $gg \to gg$ calculated through the dynamical perturbation theory [39] [31] [32], while the Heaviside function determines a threshold to

gluon mass production. In turn, the integral in brackets is the convoluted structure function for pair gluon-gluon, where using $x_2 = \tau/x_1$ we can write

$$F_{gg}(\tau) \equiv [g \otimes g](\tau) = \int_\tau^1 \frac{dx}{x}\, g(x)\, g\left(\frac{\tau}{x}\right). \tag{8}$$

We recall that $F_{gg}(\tau)$ counts the number of gluons in the colliding protons [37]. With respect the phenomenological gluon distribution we adopted the form

$$g(x) = N_g\, \frac{(1-x)^5}{x^J}\,, \tag{9}$$

with $N_g = \frac{1}{240}(6-\epsilon)(5-\epsilon)...(1-\epsilon)$ and $J = 1+\epsilon$=1.21. It is interesting to note that, due to the relation $x \simeq m_g/\sqrt{s}$, the σ_{gg} all energy dependence comes from the small x behavior of $g(x) \sim x^{-J}$, which becomes increasing important as energy increases. Hence, higher $\sqrt{s}$ means smaller x and therefore gluons with smaller momentum fractions are more abundant and this is the origin of the rising cross section in this approach [37]. Thus the gluon-gluon cross section represents the probability for the subprocess $gg \to gg$ when protons are colliding at each other.

The DGM model parameters in Eqs. (1) - (9) has been obtained in [25] carrying out a global fit to all forward pp and $p\overline{p}$ scattering data above $\sqrt{s}$= 10 GeV, namely total cross section $\sigma_{tot}^{pp,p\overline{p}}$, the ratio of the real to imaginary part of the forward scattering amplitude $\rho^{pp,p\overline{p}}$, the elastic differential scattering cross sections $d\sigma^{p\overline{p}}/dt$ at $\sqrt{s} = 546\ GeV$ and $\sqrt{s} = 1.8$ TeV as well as the TOTEM datum on σ_{tot}^{pp} at $\sqrt{s} = 7\ TeV$ [40], where we set the value of the gluon scale mass to m_g= 364 MeV [34] and fixed also the values of n_f= 4 and Λ= 284 MeV. All fitted parameters are reproduced from [25] in Table I, but now including the values of the mentioned fixed quantities (m_g, Λ, J and $\hat{\alpha}_s(0)$). The χ^2/DOF for the global fit was 0.98 for 320 degrees of freedom. We would like to emphasize that we have proceeded the analysis in [25] in order to consider the TOTEM datum on σ_{tot}^{pp} at $\sqrt{s} = 7\ TeV$, hence the parameters obtained are different from those at [31].

In order to study multiplicities we recall that the shape of P_n is so complicated that is difficult to get any analytical expression for it from solution of QCD equations [41]. However, an alternative approach is possible by studies of moments of distribution, since all moments together contain the information of the full distribution [1] and it facilitates the comparison with other models, allowing also studies of the KNO scaling hypothesis which has been an important phenomenological issue on the energy dependence of the P_n. However, a subtle

TABLE I. Values of the DGM model parameters from the global fit to the scattering pp and $\bar{p}p$ reproduced from [25]. The result was obtained by fixing the values of m_g, Λ, J and $\hat{\alpha}_s(0)$.

C_{gg}	$(1.62\pm0.37)\times10^{-3}$
μ_{gg} [GeV]	0.642 ± 0.034
A	9.04 ± 4.94
μ_{qq} [GeV]	1.299 ± 0.797
A'	$(4.68\pm1.89)\times10^{-1}$
B'	$(4.53\pm1.94)\times10^{-2}$
μ_{qg} [GeV]	$0.825\ \pm0.015$
C^-	3.12 ± 0.33
μ^- [GeV]	0.799 ± 0.298
m_g [MeV]	364
Λ [MeV]	284
J	1.21
$\hat{\alpha}_s(0)$	0.801
χ^2/DOF	0.98

problem is the proper choice of the set of moments to be adopted in the analysis (for an instructive discussion on the moments of a distribution see [42]). In this work we have adopted the standart choice and used the simple power moments, defined by

$$< n^q >= \sum_n n^q \, P_n \, , \tag{10}$$

and their scaled version

$$C_q \, = \, \frac{< n^q >}{< n >^q} \, = \, \frac{\sum n^q \, P_n}{[\sum \, n \, P_n]^q} \tag{11}$$

to parametrize P_n. Here q is a positive integer and referred to as the rank or order of the moment. The use of the average multiplicity and a few lowest C_q moments (q = 2,..,5) allows to parametrize the P_n quite satisfactorily [42]. Quantitative predictions for H_q moments oscillations were presented in [25] [29] applying the Geometrical Approach. Now, to calculate the C_q moments, Eq. (11), we have applied the so-called string model which enables linkage between the P_n and $\chi_I(s,b)$ [24] [25]. In this model P_n is decomposed into contributions

from each b with weight $1 - e^{-2\,\chi_I(s,b)}$ and written as

$$P_n(s) = \frac{\int d^2b\,\frac{[1-e^{-2\,\chi_I(s,b)}]}{f(s,b)}\,\phi^{(1)}\left(\frac{z}{f(s,b)}\right)}{< n(s) > \int d^2b\,[1 - e^{-2\,\chi_I(s,b)}]}, \tag{12}$$

where

$$f(s,b) = \xi(s)\,[\chi_I(s,b)]^{2A}\,, \tag{13}$$

$$\xi(s) = \frac{\int d^2b\,[1 - e^{-2\,\chi_I(s,b)}]}{\int d^2b\,[1 - e^{-2\,\chi_I(s,b)}]\,[\chi_I(s,b)]^{2A}}\,, \tag{14}$$

and

$$\phi^{(1)}(z) = 2\,\frac{k^k}{\Gamma(k)}\left[\frac{z}{f(s,b)}\right]^{k-1} e^{-k[\frac{z}{f(s,b)}]}\,. \tag{15}$$

$< n(s) >$ is the hadronic average multiplicity computed from experimental values using the Eq. (10), $z = n/ < n(s) >$ represents the usual KNO scaling variable. The function $\xi(s)$, Eq. (14), results from normalization condition on P_n [24], and both k and A are fitted parameters discussed in [25]. The Eq. (15) corresponds to the KNO form of the negative binomial distribution [1] and Γ is the usual gamma function. The choose of $\phi^{(1)}$, characterized by k parameter, is motivated by the fact that this distribution arises as the dominant part of the solution of the QCD equation for three gluon branching process in the very large n limit [43], allowing yet a connection between the geometrical phenomenological approach and the underlying theory of parton branching [44].

As mentioned before the string model enables linkage between P_n and χ_I and, as physical scenario, asserts that P_n in full phase space can be constructed by summing contributions from parton-parton collisions occurring at b and $\sqrt{s}$. The semihard partons produced at the interaction point fly away from each other a yielding color string, per collision, which breaks up producing the observed hadrons.

III. RESULTS AND DISCUSSION

A. Inelastic overlap functions

From Eqs. (1) - (3) we see that the eikonal function is written as the sum of the components, explicitly

$$\chi_{pp}(s,b) = \chi_{qq}(s,b) + \chi_{qg}(s,b) + \chi_{gg}(s,b) - \chi^{-}(s,b)\,. \tag{16}$$

In the eikonal representation the inelastic overlap function, $G_{in}(s,b)$, is related to the imaginary eikonal

$$G_{in}(s,b) = 1 - e^{-2\,\chi_I(s,b)} \equiv \sigma_{in}(s,b) \tag{17}$$

and it represents the probability of absorption associated to each b and $\sqrt{s}$. In view of the Eq. (16) we can express the last equation in terms of the parton components as

$$G_{in}(s,b) = 1 - e^{-2\,[\,\chi_{I\,;\,qq}(s,b) + \chi_{I\,;\,qg}(s,b) + \chi_{I\,;\,gg}(s,b) - \chi_I^-(s,b)]}. \tag{18}$$

The odd eikonal is proportional to $\frac{1}{\sqrt{s}}$, Eq. (2), and at ISR energies it represents only about 1 percent in the value of σ_{in} and therefore, as first approximation, we assume $\chi^- = 0$ in this analysis. Thus, in order to investigate the parton-parton inelastic overlap functions dependence on the $\sqrt{s}$, a phenomenological procedure is possible by fixing a component of interaction and maintaining the others equal to zero. More specifically and as example, to compute $G_{in\,;\,gg}$ we have

$$G_{in\,;\,gg}(s,b) \approx 1 - e^{-2\,\chi_{I\,;\,gg}(s,b)} \equiv \sigma_{in\,;\,gg}\,(s,b)\,, \tag{19}$$

with $\chi_{I\,;\,qq} = \chi_{I\,;\,qg} = 0$ in the Eq. (18). In a general notation

$$G_{in\,;\,ij}(s,b) \approx 1 - e^{-2\,\chi_{I\,;\,ij}(s,b)} \equiv \sigma_{in\,;\,ij}\,(s,b)\,, \tag{20}$$

with $(i,j) = (q,g)$. At this point we would like to draw attention that the Eq. (20) does not represents the partonic probability of absorption associated to each b and $\sqrt{s}$, in strict analogy to the Eq. (17). However, with this mathematical procedure we may to interpret the Eq. (20) as an associated probability with inelastic events due to the quark-quark or quark-gluon or gluon-gluon interactions taking place at b and $\sqrt{s}$, which may give important insights on partonic behavior as function of the $\sqrt{s}$ in proton interactions. Thus, within this procedure we are able to study the partonic inelastic overlap functions dependence on the collision energy, as well as the partonic inelastic cross sections.

With the QCD-inspired DGM eikonal function, Eqs. (1) - (9), and fixing the value of $b \sim 0$ we have computed $G_{in\,;\,qq}$, $G_{in\,;\,qg}$ and $G_{in\,;\,gg}$ applying the Eq. (20) and computed also G_{in} given by Eq. (18). Fig. 1 shows the results as function of $\sqrt{s}$. The probability for inelastic events by quark-quark interactions has appreciable chance of occurrence from $\sqrt{s} =$ 10 to $\sim 500\ GeV$. At ISR this probability varies from 25 to 45 percent approximately, while

the probability of gluon-gluon interactions is less then 10 percent at the same interval. Interestingly, above 100 GeV the probability for inelastic events due to gluon-gluon interactions grows rapidly with $\sqrt{s}$. From $\sqrt{s} = 100$ to 500 GeV this probability varies from ≈ 17 to more than 40 percent. At the LHC energies above 8000 GeV the probability of interactions between gluons is more than 90 percent. In turn, the quark-gluon inelastic overlap function behavior seems to indicate a slow logarithimic growth of the quark-gluon interaction activity at interval of $\sqrt{s}$ studied. The term $ln(s/m_g^2)$ in Eq. (5) can be explained by the presence of a massive gluon in the $qg \to qg$ subprocess [31]. We call attention that parton-parton scattering processes containing at least one gluon in the initial state are important to compute the QCD cross sections. In this respect and as discussed in [45], the gluon-gluon ($gg \to gg$) and quark-gluon ($qg \to qg$) scattering in fact dominate at high energies.

The UA5 Collaboration showed that the KNO scaling law was clearly broken in $p\overline{p}$ collisions at $\sqrt{s} = 546$ GeV [16] [17] and this result was confirmed also at $\sqrt{s} = 200$ and 900 GeV [18]. Related to KNO hypothesis the physical scenario that emerges in this analysis is that the fast growing of $G_{in\,;\,gg}$, above 100 GeV, increases significantly the probability of perturbative small-x gluon-gluon collisions and it may lead to the appearance of minijets. Hence, the results seems to demonstrate that the KNO violation is a consequence of the semihard contribution manifestation in the multiparticle production mechanisms, as $\sqrt{s}$ is increased. However, we should emphasize that it is not a new result from this work. In fact, in the defining the Eq. (9) the term $\sim 1/x^J$ simulates the effect of scaling violations in the small x behavior of $g(x)$ [36] [37] [38] [31], what is reflected in the present analysis.

It is worth mentioning that QCD inspired models are one of the main theoretical approaches to explain the observed increase of hadronic cross sections [46] [47] [48].

B. Inelastic cross sections

The inelastic cross section due to the imaginary eikonal can be represented by

$$\sigma_{in}(s) = \int d^2b\, G_{in}(s,b) = \int d^2b\, [\,1 - e^{-2\,\chi_I(s,b)}\,]\,. \tag{21}$$

Thus, integrating the Eq. (20) in the b plane, we obtain an associated parton-parton inelastic cross section

$$\sigma_{in\,;\,ij}(s) \approx \int d^2b\, G_{in\,;\,ij}(s,b) = \int d^2b\, [1 - e^{-2\,\chi_{I\,;\,ij}(s,b)}]\,, \tag{22}$$

which allows studies of the approximate energy dependence of the partonic cross sections. In fact, by using the χ_I given by Eqs. (1) - (9) we have obtained theoretical predictions about $\sigma_{in\,;qq}$, $\sigma_{in\,;qg}$ and $\sigma_{in\,;gg}$ dependence on the $\sqrt{s}$ within this procedure, as displayed in the Fig. 2. The inelastic cross section due to the interactions between quarks, $\sigma_{in\,;qq}$, decreases as $\sqrt{s}$ increases, at $\approx 200\ GeV$ we see that $\sigma_{in\,;qq} \to 0$, reflecting the $G_{in\,;qq}$ behavior. Above ≈ 100 GeV the gluon-gluon inelastic cross section rises fastly as function of the $\sqrt{s}$. In turn we have applied Eq. (21), which results from unitarity condition, and computed the total inelastic cross section as function of $\sqrt{s}$ with χ_I given by Eqs. (1) - (9) and by using the parameter set obtained in [25], reproduced in Table I. The result is compared with several measurements in Fig. 2, which is in very good agreement with the experimental data, specially at the highest energies where the $\chi_{gg}(s,b)$ contribution determines the asymptotic behavior of σ_{in}. It should be stressed that the σ_{in} curve in Fig. 2 has not been fit to data, and also that the σ_{in} dependence on the $\sqrt{s}$ has been determined only from fits to measurements of elastic channel observables. In addition, we have compared our results from Eq. (21) to that one from the Ref. [21] at some specific energies represented by triangles in the Fig. 3. We see that both theoretical predictions agree very well. These results are very encouraging in order to study the multiplicity distributions P_n. However, the σ_{in} results obtained in this work applying the DGM one-channel model deserves some comments. The use of one-channel models is limited and fail to simultaneously describe the total and the elastic cross section with the same parameter set [47] [48], thus multichannel models are needed to describe the diffractive component of the cross section. In this respect, it was pointed out in [48] that good descriptions of all the components of the cross section has been obtained in [49] [50] [51] and also in [52] [53] through multi-channel formulations. Now, based on the possible relation between the Poisson distribution of independent collisions and diffractive processes a suggestion was made [47] [48] that the integrand in Eq. (21) can be identified with a sum of totally independent collisions. Specifically

$$\sigma_{in}(s) = \int d^2b\,[\,1 - e^{-2\,\chi_I\,(s,b)}\,] = \int d^2b\,\left[\sum_{n=1}^{\infty} \frac{(\overline{n}_{(s,b)})^n e^{-\overline{n}_{(s,b)}}}{n!}\right], \tag{23}$$

where $\overline{n}(s,b)$ is the average number of collisions and the authors have interpreted it suggesting that the diffractive or other quasi-elastic processes might have been excluded from integration in Eqs. (21)/(23). On the basis of analysis done in this paper, we argue that de success of the DGM model to simultaneously describe total and inelastic cross sections,

with the same parameter set, may be an indication that the real part of the eikonal function, χ_R, is in fact needed in order to determine all the parameters of the eikonal model, which satisfactorily seems to describe the full inelastic cross section through the entire available $\sqrt{s}$ interval. Thus, the present result on σ_{in} is a straightforward consequence of the overall parameter fitting of the total cross section, the ratio of the real to imaginary part of the forward scattering amplitude and the differential cross section.

Due to the mentioned limitations on the application of the one channel approaches [50] it seems instructive show how the one-channel DGM model can be used to predict the ratio between the elastic and total cross sections, σ_{el}/σ_{tot}, which provides crucial information on the asymptotic properties of the hadronic interactions [54]. We have used the equations given by

$$\sigma_{el}(s) = \int d^2b \, | \, 1 - e^{-\chi_I(s,b) + i\,\chi_R(s,b)} |^2 \, , \tag{24}$$

$$\sigma_{tot}(s) = 2 \int d^2b \, [\, 1 - e^{-\chi_I(s,b)} \, Cos\chi_R(s,b)] \, , \tag{25}$$

to compute this physical quantity. The results of the computation are displayed in Fig. (4) and reproduces with a good approximation the experimental information compiled in [54].

C. C_q moments

Some characteristics of P_n can be quantified in terms of the scaled version of the simple power moments, Eq. (11). Thus, we have calculated both theoretical and experimental C_q moments for full phase space P_n over a large range of energies where there are available experimental data, namely at $\sqrt{s} = 30.4, 44.5, 52.6, 62.2, 300, 546, 1000$ and $1800\ GeV$ [15] [19]. For energies $\sqrt{s} \geq 300\ GeV$ we used P_n data from the E735 Collaboration since it is statistically more reliable in the high multiplicity region [19]. Theoretical P_n values were obtained by using the mentioned string model, Eqs. (12) - (15) with χ_I given by Eqs. (1) - (9). Our theoretical and experimental results on C_q are summarized in Table II and compared with the Figure 5 (for q=2,3) and Figure 6 (for q=4,5), indicating that the KNO scaling is approximately valid at ISR energies but with clear indication that it is broken above $\approx 100\ GeV$. At the LHC energies from $\sqrt{s} = 7000$ to $14000\ GeV$ the theoretical results predicts strong violation of the scaling, in qualitative agreement with the results reported by CMS Collaboration, albeit in pseudorapidity interval of $|\eta| < 2.4$ [6].

We recall that the C_q moments depends uniformly on the probabilities and in its calculation the lowest multiplicities are suppressed and the high multiplicity tail is enhanced. Thus, our results reflects the influence of the tail of the distributions.

IV. CONCLUDING REMARKS

Applying a phenomenological procedure in which the eikonal is written as the sum of quark-quark, quark-gluon and gluon-gluon contributions, we present theoretical predictions for both inelastic cross section and C_q moments of P_n for pp interactions. The comparisons of predictions with a variety of published data shows good agreement. The imaginary eikonal $\chi_I(s,b)$ energy dependence, and hence of the σ_{in}, has been completely determined only from elastic fit. The P_n values has been obtained by adopting an approach which enables linkage between the elastic and inelastic channels thought unitarity condition of the S-matrix. Our mathematical procedure allows studies of the parton-parton inelastic cross sections, $\sigma_{in\,;ij}$, dependence on $\sqrt{s}$, as well as partonic inelastic overlap function, $G_{in\,;ij}$, where $(i,j) = (q,g)$. Based on the approximate results on the collision energy dependence of $G_{in\,;ij}$, we have discussed the violation of KNO scaling as a possible consequence of the manifestation of semihard partons in the particle production mechanism. At the LHC energies our results predicts strong violation of the KNO hypothesis. This result is in agreement with several experimental and theoretical previous studies developed on the subject. The limited use of the one-channel eikonal approach to simultaneously describe the total and the elastic cross sections has been briefly discussed and prediction to the ratio σ_{el}/σ_{tot} as function of $\sqrt{s}$ is presented and compared with the data. Despite some simplifications made in our procedure, reflecting only approximate results on the collision energy dependence of the partonic inelastic cross sections and overlap functions, we believe that the results may serve as guidance for a theoretical understanding of the cross sections behavior in terms of the proton components. An interesting result of this analysis is that we have a clear idea on the approximate behavior of the parton-parton components as function of the collision energy in proton interactions.

ACKNOWLEDGMENTS

I am thankful to M.J. Menon and E.G.S. Luna for helpful discussions and suggestions. I thank to P.V.R.G. Silva, M.J. Menon and D.A. Fagundes for the permission to use the experimental data compiled in [54]. I am also thankful to two anonymous referees for valuable comments, suggestions and discussions.

TABLE II. Experimental data with error bar and theoretical C_q values calculated in this work by using the Eqs. (10) - (15). Data points for P_n from [15] [19].

$\sqrt{s}$ - GeV	C_2	C_3	C_4	C_5
30.4	1.29 ± 0.05	1.97 ± 0.09	3.45 ± 0.21	6.68 ± 0.52
	1.27	1.93	3.35	6.48
44.5	1.28 ± 0.04	1.95 ± 0.07	3.40 ± 0.17	6.58 ± 0.47
	1.28	1.94	3.38	6.55
52.6	1.29 ± 0.03	1.98 ± 0.06	3.48 ± 0.15	6.81 ± 0.42
	1.28	1.95	3.40	6.63
62.2	1.29 ± 0.03	1.97 ± 0.06	3.40 ± 0.14	6.43 ± 0.33
	1.27	1.91	3.28	6.24
300	1.34 ± 0.02	2.21 ± 0.04	4.26 ± 0.07	9.23 ± 0.17
	1.35	2.23	4.27	9.20
546	1.41 ± 0.03	2.52 ± 0.05	5.31 ± 0.10	12.72 ± 0.24
	1.43	2.57	5.41	12.88
1000	1.41 ± 0.02	2.47 ± 0.05	5.11 ± 0.13	11.87 ± 0.36
	1.42	2.49	5.11	11.74
1800	1.47 ± 0.02	2.78 ± 0.03	6.23 ± 0.07	15.91 ± 0.21
	1.48	2.79	6.20	15.63
7000	1.58	3.19	7.46	19.21
8000	1.60	3.25	7.69	20.06
13000	1.65	3.51	8.71	23.88
14000	1.66	3.60	9.16	25.91

[1] Jan Fiete Grosse-Oetringhaus and Klaus Reygers, J. Phys. G: Nucl. Part. Phys. **37**, 083001 (2010); arXiv:0912.0023 [hep-ex], (2009) .

[2] S.M. Troshin and N.E. Tyurin, J.Phys. G: Nucl. Part. Phys. **29**, 1061 (2003).

[3] M. Froissart, Phys. Rev. **123**, 1053 (1961);

[4] A. Martin, Nuovo Cimento **42** 930; **44** 1219 (1966);

[5] A. Martin, Phys. Rev. D **80**, 065013 (2009).

[6] CMS Collaboration, JHEP **1101**, 079, (2011); arXiv:1011.5531[hep-ex], (2010).

[7] G. Aad *et al.*, ATLAS Coll., Nat. Commun. 2:463 (2011).

[8] B. Abelev *et al.*, ALICE Coll., Eur. Phys. J. C **73**, 2456 (2013).

[9] G. Antchev *et al.*, TOTEM Coll., Eur. Phys. Lett. 101, 21004 (2013).

[10] G. Antchev *et al.*, TOTEM Coll., Phys. Rev. Lett. 111, 012001 (2013).

[11] G. Antchev *et al.*, TOTEM Coll., Eur. Phys. Lett. 101, 21003 (2013).

[12] S. Chatrchyan *et al.*, CMS Coll., Phys. Lett **722**, 5 (2013).

[13] LHCb Coll., JHEP02 **129**, (2015); arXiv:1412.2500 (2015).

[14] U. Amaldi and K.R. Schubert, Nucl. Phys. B **166**, 301 (1980).

[15] A. Breakstone *et al.*, ABCDWH Coll.,Phys. Rev. D **30**, 528 (1984).

[16] G.J. Alner, *et al.*, Phys. Lett. B **138**, 304 (1984).

[17] G.J. Alner, *et al.*, UA5 Coll., Phys. Rep. **154**, (5-6) 247 (1987).

[18] R.E. Ansorge, *et al.*, Z. Phys. C - Particles and Fields **43**, 357 (1989).

[19] T. Alexopoulos *et al.*, E735 Coll., Phys. Lett. B **435**, 453 (1998).

[20] S.L.C. Barroso, *et al.*, Nucl. Phys. B (Proc. Suppl.) **75**, 150 (1999).

[21] A.K. Kohara, E. Ferreira and T. Kodama, Eur. Phys. J. C **74**, 3175 (2014). arXiv:1408.1599 [hep-ph].

[22] A. Giovannini and R. Ugoccioni, Nucl. Phys. B (Proc. Suppl.) **64**, 68 (1998).

[23] C.S. Lam and P.S. Yeung, Phys. Lett. B **119**, 445 (1982).

[24] P.C. Beggio, M.J. Menon, and P. Valin, Phys. Rev. D **61**, 034015 (2000).

[25] P.C. Beggio and E.G.S. Luna, Nucl. Phys. A **929**, 230 (2014).

[26] P.C. Beggio and Y. Hama, Braz. J. Phys, **37**, 1164 (2007).

[27] P.C. Beggio, Braz. J. Phys, **38**, 598 (2008).

[28] P.C. Beggio, Nucl. Phys. A **864**, 140 (2011).

[29] P.C. Beggio, Nucl. Phys. A **913**, 264 (2013).

[30] Saul Barshay and Dieter Rein, Phys. Lett. B **218**, 337 (1989).

[31] E.G.S. Luna, A.F. Martini, M.J. Menon, A. Mihara, A.A. Natale, Phys. Rev. D **72**, 034019 (2005).

[32] E.G.S. Luna, A.A. Natale, Phys. Rev. D **73**, 074019 (2006).

[33] D.A. Fagundes, E.G.S. Luna, M.J. Menon, and A.A. Natale, Nucl. Phys. A **886**, 48 (2012).

[34] E.G.S. Luna, A.L. dos Santos, and A.A. Natale, Phys. Lett. B **698**, 52 (2011); E.G.S. Luna, Phys. Lett. B **641**, 171 (2006).

[35] Y. Afek, C. Leroy, B. Margolis, P. Valin, Phys. Rev. Lett. **45** 85 (1980);
T.K. Gaisser, F. Halzen, Phys. Rev. Lett. **54** 1754 (1985);
P. LHeureux, B. Margolis, P. Valin, Phys. Rev. D **32** 1681 (1985);
G. Pancheri, Y. Srivastava, Phys. Lett. B **159** 69 (1985);
L. Durand and H. Pi, Phys. Rev. Lett. **58** 303 (1987);
L. Durand and H. Pi, Phys. Rev. Rev. D **40** 1436 (1989);
M. Block, R. Fletcher, F. Halzen, B. Margolis and P. Valin, Phys. Rev. D **41** 978 (1990);

[36] B. Margolis, P. Valin, M.M. Block, F. Halzen and R.S. Fletcher, Phys. Lett. B **213** 221 (1988).

[37] Martin Block, Robert Fletcher, Francis Halzen, Bernard Margolis and Pierre Valin, Nucl. Phys. B (Proc. Suppl.) **12**, 238 (1990).

[38] M.M. Block, E.M. Gregores, F. Halzen and G. Pancheri, Phys. Rev. D **60**, 054024 (1999).

[39] H. Pagels and S. Stokar, Phys. Rev. D **20**, 2947 (1979).

[40] G. Antchev, *et al.*, Europhys. Lett. **101**, 21002 (2013).

[41] I.M. Dremin, Phys. At. Nucl. **68** (5), 758 (2005).

[42] K. Fialkowski and R. Wit, Acta Phys. Pol. B **42**, No 2, 293 (2011).

[43] B. Durand and I. Sarcevic, Phys. Lett. B **172**, 104 (1986); Phys. Rev. D **36**, 2693 (1987).

[44] S. Barshay and J. Goldberg , Phys. Lett. B **196**, 566 (1987); Phys. Rev. Lett. **49**, 1609 (1982).

[45] C.A.S. Bahia, M. Broilo and E.G.S. Luna, Phys. Rev. D **92**, 074039 (2015); J. Phys. Conf. Ser. **706** 052006 (2016).

[46] A. Corsetti, A. Grau, G. Pancheri, and Y.N. Srivastava, Phys. Lett. B **382**, 282 (1996);
A. Grau, G. Pancheri, and Y.N. Srivastava, Phys. Rev. D **60**, 114020 (1999);
R.M. Godbole, A. Grau, G. Pancheri, and Y.N. Srivastava, Phys. Rev. D **72**, 076001 (2005);

A. Achilli *et al.*, Phys. Lett. B **659**, 137(2008);

A. Grau, R.M. Godbole, G. Pancheri, and Y.N. Srivastava, Phys. Lett. B **682**, 55 (2009);

[47] D.A. Fagundes, G. Pancheri, A. Grau, S. Pacetti and Y.N. Srivastava, Phys. Rev. D **88**, 094019 (2013); arXiv:1306.0452 [hep-ph].

[48] D.A. Fagundes, A. Grau, G. Pancheri, Y.N. Srivastava and O. Shekhovtsova, Phys. Rev. D **91**, 114011 (2015); arXiv:1504.04890 [hep-ph].

[49] V. Khoze, A. Martin and M. Ryskin, Eur. Phys. J. **C74**, 2756 (2014). arXiv:1312.3851 [hep-ph].

[50] P. Lipari and M. Lusignoli, Phys. Rev. D **80**, 074014 (2009); arXiv:0908.0495 [hep-ph].

[51] P. Lipari and M. Lusignoli, Eur. Phys. J. **C73**, 2630 (2013). arXiv:1305.7216 [hep-ph].

[52] E.G.S. Luna, V.A. Khoze, A.D. Martin and M.G. Ryskin, Eur. Phys. J. **C59**, 1 (2009).

[53] E.G.S. Luna, V.A. Khoze, A.D. Martin and M.G. Ryskin, Eur. Phys. J. **C69**, 95 (2010).

[54] D.A. Fagundes, M.J. Menon and P.V.R.G. Silva, Nucl. Phys. A **946**, 194 (2016).

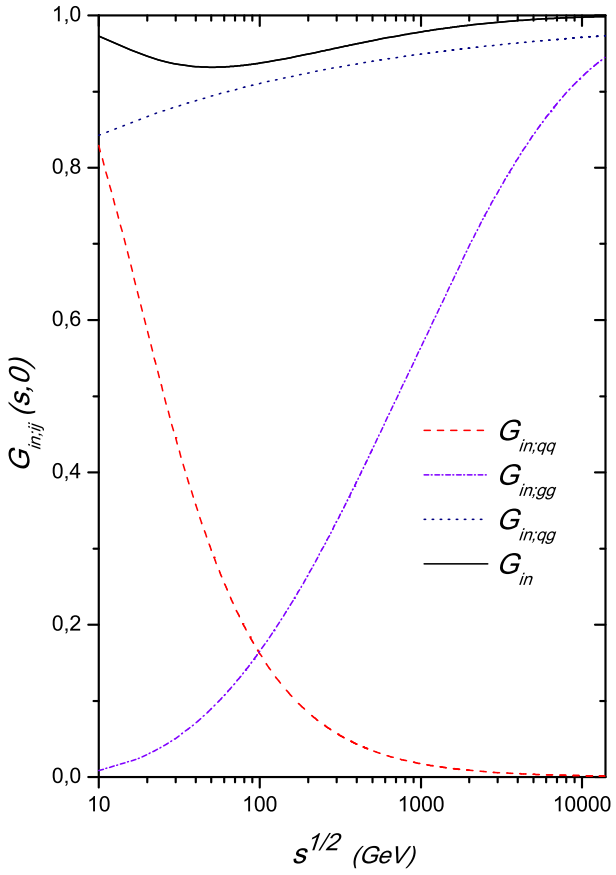

FIG. 1. The approximate collision energy dependence of the quark-quark, quark-gluon and gluon-gluon inelastic overlap functions calculated by using the Eq. (20) at $b \sim 0$, as explained in the text. The solid line represents the result for G_{in} obtained with the Eq. (18).

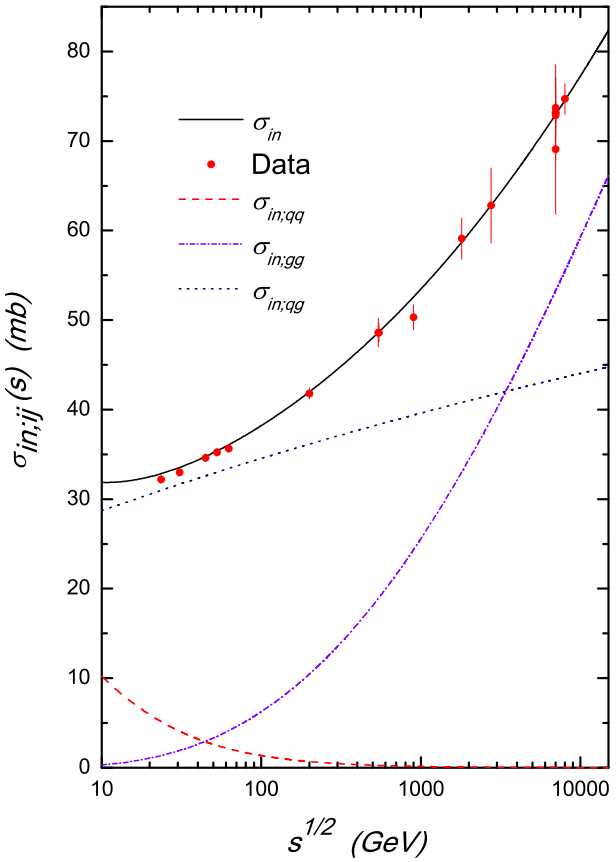

FIG. 2. Theoretical predictions as a function of $\sqrt{s}$ for quark-quark, quark-gluon and gluon-gluon inelastic cross sections, Eq. (22). The solid line represents the total inelastic cross section, Eq. (21), compared with a variety of data points from [7] [8] [9] [10] [11] [14] [15].

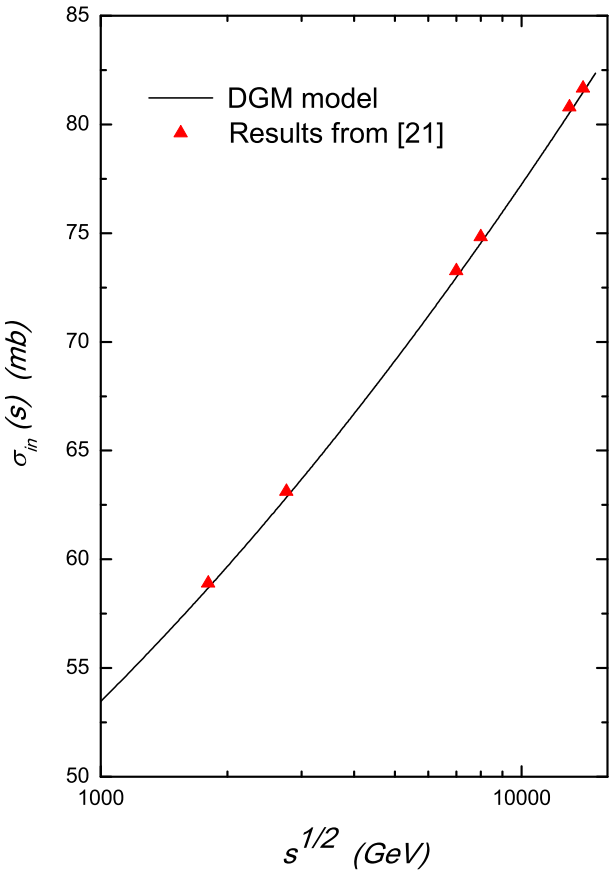

FIG. 3. Comparison between our calculations for pp inelastic cross section (solid line) with the predictions from model discussed in [21] at $\sqrt{s}$ of 1800, 2760, 7000, 8000, 13000 and 14000 GeV (triangles).

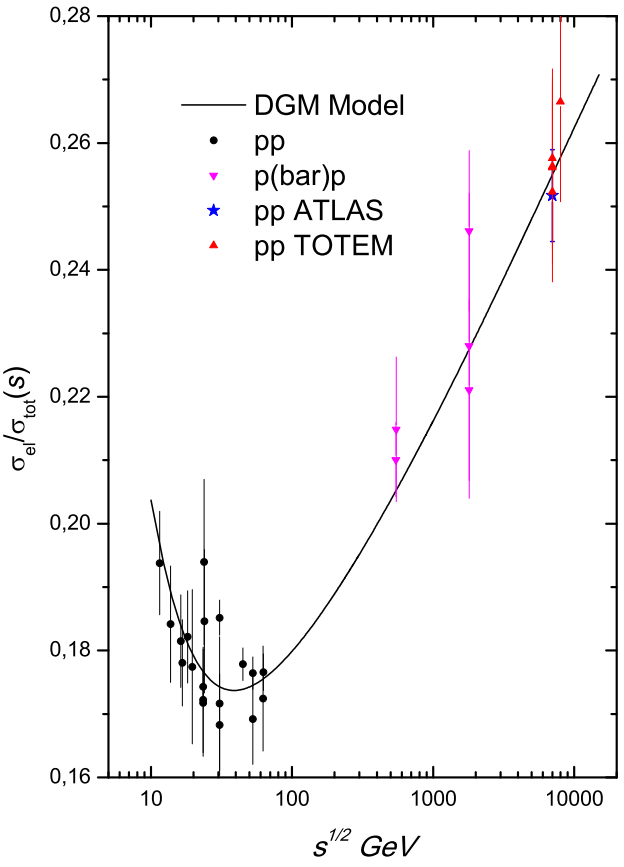

FIG. 4. DGM model prediction on the ratio σ_{el}/σ_{tot} by using the parameter set reproduced from [25], Table I. Experimental data are from *pp* scattering as compiled at [54].

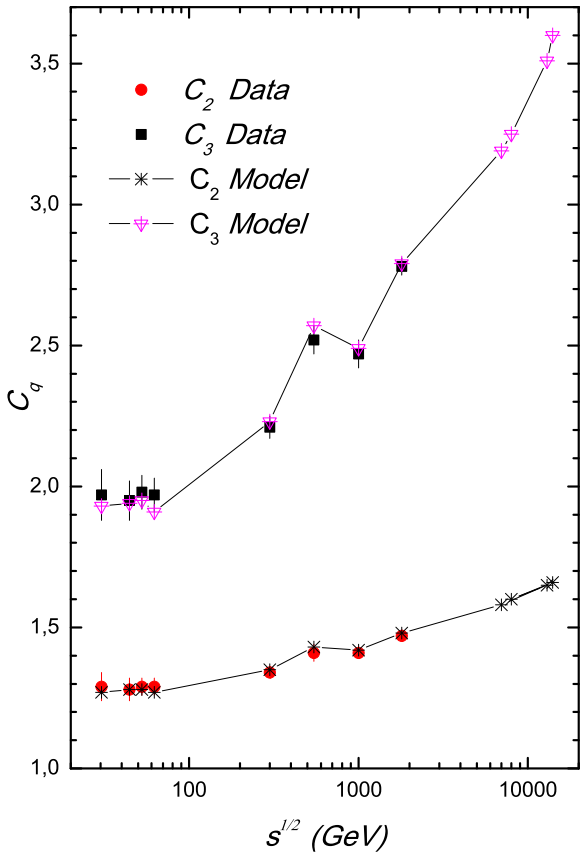

FIG. 5. Theoretical and experimental C_q moments, q=2,3, calculated in this work in full phase space using the Eq. (11). Theoretical values of P_n were obtained applying the Eqs. (12) - (15) with the imaginary eikonal χ_I given by Eqs. (1) - (9). Experimental P_n values are from [15] [19] and the lines are draw only as a guidance of the theoretical points.

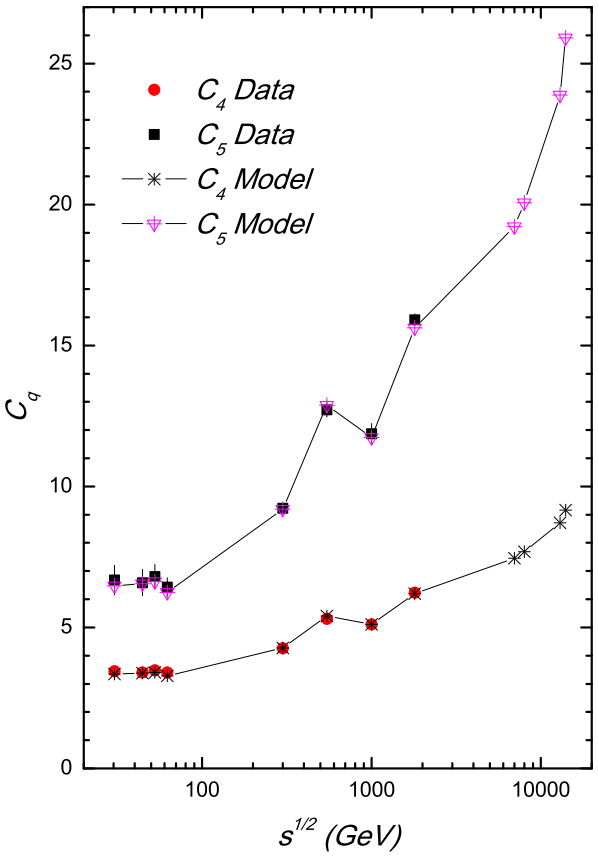

FIG. 6. Same as Figure 5 but for q=4,5.